

# Dynamic Modeling of Soft Manipulators Actuated by Twisted-and-Coiled Actuators\*

Ben Pawlowski, Jiefeng Sun, and Jianguo Zhao

**Abstract**—Soft robots—robots made of soft materials—have strong potential for applications where traditional rigid robots are not suitable (e.g., safely collaborating with humans). However, actuation methods for most existing soft robots still require rigid components to function, and when they do not, they have a limited range of forces and displacements. A new artificial muscle, Twisted-and-Coiled actuators (TCAs), may provide partial solutions to this. They are capable of producing large forces and deformations comparable to or superior to human muscles. However, the dynamic modeling for TCAs when embedded inside soft materials is not trivial due to the coupling of deformations between the actuators and the body. In this paper, we model the dynamics for the thermally driven actuation and extend a dynamic Cosserat rod model to describe the dynamics of the soft body. We also numerically simulate the model to test its correctness. The proposed model is a generalization of existing models and can be applied to the modeling of soft robots when couplings exist between the actuator and the soft body.

## I. INTRODUCTION

Soft robots can leverage the compliance of flexible materials to be more adaptable and safer than traditional rigid robots [1]. For instance, soft manipulators can readily adapt to uncertain environments, provide safer equipment for use in medical devices [2], [3], and have the potential to be used in situations when rigid manipulators may fail (e.g., high impact scenarios [4], required large deformations, etc.). Soft manipulators are more adaptable when grasping, contacting, and avoiding objects relative to rigid ones. These advantages have led to the development of a variety of manipulators, which commonly take some biological inspiration such as elephant trunks [5] and octopus arms [6], [7], [8]. Some of the major difficulties for soft robots are how to best actuate the manipulator and dealing with the complications in kinematic and dynamic modeling due to infinite degrees of freedom in the soft and compliant bodies.

There have been many approaches to actuate soft robots. The most common strategies among these are cables/tendons [7], [9], pneumatics [6], and smart materials such as shape memory alloys (SMAs) [10], Ionic-Polymer/Metal Composites (IPMCs) [11], and Dielectric-Elastomer Actuators (DEAs) [12]. For actuation with cables and pneumatics, it is necessary to have external components to provide the actuation (e.g., motors and pumps) that force

some portion of the system to no longer be compliant and unnecessarily make the manipulators bulky. Smart materials can be simply actuated by applied voltages, but they in general suffer from high manufacturing costs [13] and low force generations.

We recently proposed to actuate soft robots with twisted-and-coiled actuators (TCAs), a new type of artificial muscle that can be produced from low-cost sewing thread. TCAs made from conductive sewing threads can be actuated by directly applying electricity and can generate more than 100 times the force a human muscle of the same weight [14]. Compared with other artificial muscles, TCAs are low cost and can be easily fabricated through the twisting and coiling of threads. Further, TCAs are able to generate either extension or contraction force determined by the coiling directions, and the actuation force can be tuned by changing the spring index. TCAs can be actuated with an applied voltage through Joule heating, thus requiring minimal external components for their actuation. Therefore, TCAs pose a promising strategy to actuate soft robots in a cheap and easy-to-manufacture way that needs minimal external components to operate.

However, a major difficulty with TCAs comes from modeling their behavior when embedded in soft materials. The force generated by a TCA depends on both its temperature and its deformation [15]. If a TCA is embedded inside a soft material, its deformation will be coupled with the material's deformation, which will in turn be determined by the force generated by the TCA. As a result, we need to consider the modeling of soft bodies and the embedded TCAs simultaneously, complicating the modeling process. The result of this coupling is that existing static and dynamic models of soft robots do not fully capture the behavior and have to be extended to properly model a manipulator driven by TCAs.

Various modeling methods for soft or compliant robots have been proposed recently. The most typical method assumes a slender body (i.e., the body length is much longer than its width), allowing for the usage of rod or beam models. In these rod models, it is common to make a constant curvature (CC) approximation [16], [8], which assumes that the manipulator has a circular shape and allows for modeling strategies from rigid robots (e.g., DH-parameters). However, this assumption limits the model to being static with negligible external forces. Other approaches include extensions to the CC model, such as piecewise constant curvature (PCC) [17] and the discrete Cosserat rod approach [18]. Other non-discrete approaches use other rod

\*This work is partially supported by the National Science Foundation under Grant IIS-1755766.

Ben Pawlowski, Jiefeng Sun, and Jianguo Zhao are with the Department of Mechanical Engineering, Colorado State University benpawski@rams.colostate.edu, J.Sun@colostate.edu, and Jianguo.Zhao@colostate.edu

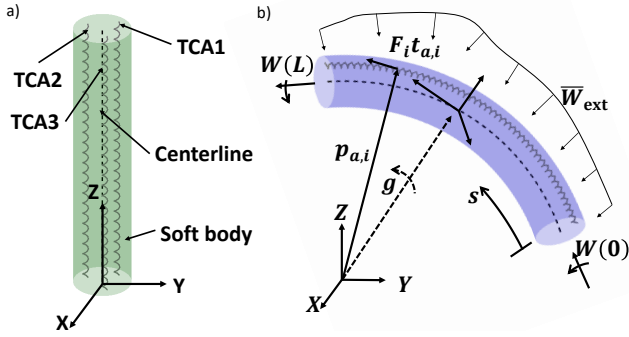


Fig. 1. a) An example of a manipulator investigated in this paper. It is composed of three TCAs embedded inside a circular soft body. They are placed symmetrically around the center and separated by an angle of  $120^\circ$ . b) The setup for analyzing a Cosserat rod, here a single embedded TCA is shown in gray.

and beam theories like Euler-Bernoulli beam theory [10], Kirchoff rod theory [19], and Cosserat rod theory [20], [21], which is the most general theory capable of modeling most phenomena in soft robots. However, these models are nonlinear and typically have no analytic solution and must be numerically solved. Finite element analysis (FEA) has also been used for modeling [2] cases where rods are not a good approximation. The general trade-off is that the constant strain assumption reduces the computational complexity at the cost of accuracy and ability to capture more complex interactions.

In this paper, we will address the dynamics modeling for soft robots actuated by conductive TCAs by combining a thermodynamic model and a dynamic Cosserat rod model. The thermodynamic model is necessary to predict the temperature of TCAs given an applied voltage. The thermodynamics will treat each TCA embedded inside a soft body as a resistive heat source diffusing heat through the body. Then, a dynamic Cosserat rod model [21] will be leveraged to analyze the dynamic response of the robot by considering the coupling of TCAs and the soft body. Integrating the thermodynamics and the dynamic Cosserat rod model, we can obtain the full forward dynamics, going from input voltage to the manipulator motion. Such a modeling framework will lay a theoretical foundation for using TCAs to enable dynamic, miniature, and untethered soft robots.

The rest of this paper is organized as follows. In section II, we present the thermodynamic modeling and the mechanics of the manipulator. Then, in section III, we simulate the dynamic models and discuss the simulation results. In the final section, we discuss our conclusions and future work.

## II. MODELING

Without loss of generality, we will analyze a soft manipulator shown in Fig. 1a. It is comprised of a soft body and three TCAs separated radially by  $120^\circ$ . The TCAs are fabricated using conductive sewing thread, so that they may be heated through an applied voltage via Joule heating. Further, they are fabricated to serve as extension muscles

to eliminate the pre-stretch required by contraction muscles. Three TCAs are chosen as that is the minimum number to generate three-dimensional motion. The main feature to note with this manipulator is that the length is much larger than the diameter, which will be used for approximations later in the thermal modeling and the mechanics modeling. We place the fixed frame at the base of the manipulator with the  $z$ -axis being vertical and the  $x$  and  $y$ -axes aligned with the TCAs as shown in Fig. 2.

The goal for the modeling is to be able to predict the thermal profile and motion of the manipulator given input voltages to the TCAs. Our only input is voltage as we are using conductive TCAs which will generate heat when a voltage is applied and the resulting temperature change in the TCAs actuate them [15]. Then, once the thermal profile is determined for the body and TCAs, the temperatures of the TCAs can be used as inputs into the dynamics to determine the motion the manipulator.

In the rest of this section, we first develop the thermal model by treating the TCAs as a heat source and incorporate conduction through the body with convection at the exposed surface. Since the body of the manipulator has a much longer length than its diameter, we only analyze a cross section rather than the entire body. Due to the asymmetry in the system, it is necessary to numerically solve the relevant heat equation. Next, we model the soft body as a Cosserat rod. With the rod model, we develop the dynamic equations and incorporate the coupling between the body and the embedded TCAs. This also requires us to numerically solve a system of partial differential equations (PDEs).

### A. Thermal Model

The TCAs are driven by heat stimulus from electricity passing through them. The temperature of a TCA will determine its output force and displacement. In order to predict the motion of a soft manipulator, we need to establish a thermal model to relate the input voltage with the temperature of the TCA.

Fig. 2 shows a cross section of the soft manipulator. The transient temperature distribution field on the cross section is governed by the following heat diffusion equation [22]

$$\frac{\partial}{\partial x} \left( k \frac{\partial T}{\partial x} \right) + \frac{\partial}{\partial y} \left( k \frac{\partial T}{\partial y} \right) + \dot{q}(t, x, y) = \rho c_p \frac{\partial T}{\partial t} \quad (1)$$

where  $T$  is temperature distribution throughout the material,  $\dot{q}$  is heat flux of the material, a function varying with time  $t$ .  $k$ ,  $\rho$ , and  $c_p$  are the thermal conductivity, mass density, and specific heat of the material, respectively. The heat flux value,  $\dot{q}$ , depends on the region of the manipulator. If  $(x, y)$  is in the body region, then  $\dot{q} = 0$ , and if  $(x, y)$  is in the region of a TCA, then  $\dot{q} = \dot{q}_i$ , where  $i$  indicates the  $i$ -th TCA.

The external force exerted on the TCA [23] will influence its electrical resistance; however, for our range of forces the resulting change in resistance is roughly  $0.1\Omega$  (a 1% change) so we neglect this effect. We also treat the TCA as a tube

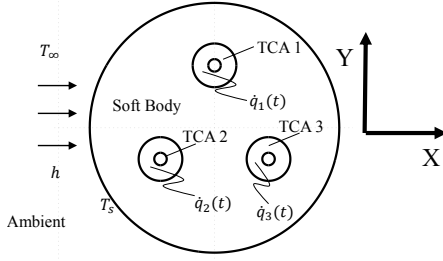


Fig. 2. Schematic of the 2D thermal model of the soft manipulator.

with the diameter of the twisted precursor fiber as the wall thickness because at the reference configuration, the coils are all touching and at most the gaps between the coils would be 0.05 mm, making their influence negligible. Thus, the body heat flux of a TCA is [22]

$$\dot{q}_i(t) = \frac{4V_i(t)^2}{R_0 l^2 \pi (D^2 - d^2)}, i = 1, 2, 3 \quad (2)$$

where  $V_i(t)$  is the voltage applied to the  $i$ th TCA, which is our control input.  $R_0$  is resistance of a unit length of the TCA,  $l$  is the length of a single TCA,  $D$  is the outer diameter of the TCA, and  $d$  is the inner diameter of the TCA.

The motion of the soft manipulator will influence the heat dissipation rate of the soft body, but the velocity will not exceed 0.1 m/s, allowing us to assume the convection coefficient is constant [22]. So we can use a constant convective heat transfer coefficient to specify convective heat transfer through the boundary, namely the circular perimeter of the cross section in contact with ambient fluid media (gas or liquid) [22]:

$$k \left( \frac{\partial T}{\partial x} + \frac{\partial T}{\partial y} \right) = h(T - T_\infty) \quad (3)$$

where  $T$  is the temperature distribution on the boundary,  $T_\infty$  is the ambient temperature, and  $h$  is the convective heat transfer coefficient.

Since the inner diameter of the TCA is very small (0.4 mm), we assume the inner surface of the TCA is an adiabatic surface because with such a small size, the internal temperature distribution must be uniform and equal to the temperature of the inner wall, leading to no heat transfer. Also, due to the maximum temperature of the soft manipulator's surface being fairly low (less than 100°C), we ignore energy loss from radiation. The parabolic partial differential equations and the boundary conditions presented above can be solved with Matlab's PDE toolbox. The TCA's temperature at a certain time can be derived by averaging the temperatures at all nodes in the TCA region.

With the thermal model, we can predict the behavior of the TCAs. The working principle for TCAs is that thermal-induced radial expansion will cause untwisting in these fibers to generate an untwist torque, which will become an axial force along the TCA. The characterizing equation for the TCA behavior is derived in [15] and is:

$$\delta = f_1 F + f_2 \tau(T) \quad (4)$$

where  $\delta$  is the TCA's displacement,  $F$  is the force generated along the TCA's body,  $\tau(T)$  is the generated torque with a dependence on temperature  $T$ , and the coefficients  $f_1$  and  $f_2$  are derived from Castigliano's Second theorem, the forms of which can be found in [15].

### B. Dynamics Modeling

A Cosserat rod is a way of modeling a slender body by assuming that the object may be described with a single spatial dimension  $s \in [0, L]$ , where  $L$  is the length of the body in the reference configuration [21]. A diagram of the setup for a Cosserat rod can be seen in Fig. 1b. This spatial dimension is referred to as the material abscissa, which is the line that runs through the centroid of every cross section in the body or the centerline of the body. At every point along the centerline there exists an orthonormal body frame, typically referred to as the directors, and a transformation from a fixed frame to this body frame can be described by a homogeneous transform  $g$  comprised of a rotation,  $R$ , and a position,  $\mathbf{p}$ , this transformation describes the configuration of the body through space and time. The rates of change for  $g$  with respect to space,  $s$ , and time,  $t$ , are:

$$\frac{\partial g}{\partial s} \triangleq g' = g \hat{\xi} = \begin{bmatrix} R & \mathbf{p} \\ \mathbf{0} & 1 \end{bmatrix} \begin{bmatrix} \hat{\kappa} & \lambda \\ \mathbf{0} & 0 \end{bmatrix} \quad (5)$$

$$\frac{\partial g}{\partial t} \triangleq \dot{g} = g \hat{\eta} = \begin{bmatrix} R & \mathbf{p} \\ \mathbf{0} & 1 \end{bmatrix} \begin{bmatrix} \hat{\omega} & \mathbf{v} \\ \mathbf{0} & 0 \end{bmatrix} \quad (6)$$

where  $\hat{\cdot}$  denotes the derivative with respect to  $s$  and  $\dot{\cdot}$  the derivative with respect to time.  $\xi \in \mathbb{R}^6$  represents the strain vector, or spatial twist, for the body and it is comprised of the angular strains,  $\kappa \in \mathbb{R}^3$ , and the linear strains,  $\lambda \in \mathbb{R}^3$ .  $\eta \in \mathbb{R}^6$  is the velocity of the rod at a point  $s$ , or temporal twist, and is comprised of the angular velocities,  $\omega \in \mathbb{R}^3$ , and the linear velocities,  $\mathbf{v} \in \mathbb{R}^3$ . The operator  $\hat{\cdot}$  represents both the transformation from  $\mathbb{R}^3$  to  $se(3)$  and  $\mathbb{R}^6$  to  $SE(3)$ . Another operator  $\check{\cdot}$  will also be used to represent the inverse transformation for  $\hat{\cdot}$ . For the wrench balance, we require that the time rate of change of a cross section's momentum,  $\gamma$ , balance with the internal wrench,  $\mathbf{W}_{int}$ , across the cross section and the external distributed wrench at the cross section,  $\bar{\mathbf{W}}_{ext}$ . A wrench is the combination of a moment and a force and represented as  $\mathbf{W} = [moment, force]^T$ . This may be written as [21]:

$$\frac{\partial}{\partial s} \mathbf{W}_{int} + \bar{\mathbf{W}}_{ext} = \frac{\partial}{\partial t} \gamma \quad (7)$$

where  $\gamma = \Gamma \eta$  and  $\Gamma = \rho \text{diag}(I_x, I_y, J, A, A, A)$ .  $\Gamma$  is the inertia matrix of a cross section with  $\rho$  the density,  $I_x$  and  $I_y$  the second area moments of inertia about the  $x$  and  $y$  axes,  $J$  the polar moment of inertia, and  $A$  the area of the cross section.

Then, using the fact that wrenches and twists form a Lie Algebra, the balance can be expanded out to [21]:

$$\mathbf{W}'_{int} - ad_{\xi}^* \mathbf{W}_{int} + \bar{\mathbf{W}}_{ext} = \Gamma \dot{\boldsymbol{\eta}} - ad_{\boldsymbol{\eta}}^* \Gamma \boldsymbol{\eta} \quad (8)$$

the  $ad_{\xi}^*$  and  $ad_{\boldsymbol{\eta}}^*$  are the coadjoint maps and are the transposes of the adjoint maps defined as:

$$ad_{\xi} = \begin{bmatrix} \hat{\boldsymbol{\kappa}} & 0 \\ \hat{\boldsymbol{\lambda}} & \hat{\boldsymbol{\kappa}} \end{bmatrix}, \quad ad_{\boldsymbol{\eta}} = \begin{bmatrix} \hat{\boldsymbol{w}} & 0 \\ \hat{\boldsymbol{v}} & \hat{\boldsymbol{w}} \end{bmatrix} \quad (9)$$

Then, using Eqs. (5) and (6), it is possible to derive the rate of change for the strain,  $\boldsymbol{\xi}$ , with respect to time. To do this, we use the fact that partial derivatives can be done in arbitrary order (i.e.,  $\frac{\partial}{\partial t} \frac{\partial g}{\partial s} = \frac{\partial}{\partial s} \frac{\partial g}{\partial t}$ ). So, we take the derivatives of Eqs. (5) and (6) to get  $\dot{g}'$  and set the results equal to each other to get:

$$\dot{\boldsymbol{\xi}} = \boldsymbol{\eta}' + ad_{\xi} \boldsymbol{\eta} \quad (10)$$

Next, we look at how to model the internal wrench of the body. In the simplest case, the body only has an associated stiffness and no viscosity. In general, it is necessary to incorporate both stiffness and viscosity into the model and a common way is with a **Kelvin-Voigt model [24]**; however, for exposition it is not necessary to incorporate all the material properties as they can be included later.

The internal stiffness can be formulated as:

$$\mathbf{W}_{int} = K(\boldsymbol{\xi} - \boldsymbol{\xi}^*) \quad (11)$$

where  $K = \text{diag}(EI_x, EI_y, GJ, GA, GA, EA)$  is the stiffness matrix with  $E$  as the Young's modulus and  $G$  as the shear modulus. This assumes that the body frame is always aligned with the principal axes and that only a linear elastic model is necessary for the body material. Also,  $\boldsymbol{\xi}^*$  is the strain in the reference configuration. In the case where the body is initially straight, we have  $\boldsymbol{\xi}^* = [0, 0, 0, 0, 0, 1]^T$ .

The distributed external wrench,  $\bar{\mathbf{W}}_{ext}$ , comes from the wrench generated due to the actuators and other external wrenches, such as gravity. Thus it may be broken down as:

$$\bar{\mathbf{W}}_{ext} = Ad_g^* (\bar{\mathbf{W}}_{act} + \bar{\mathbf{W}}_e) \quad (12)$$

$$\text{with } Ad_g^* = \begin{bmatrix} R^T & -R^T \hat{\boldsymbol{p}} \\ 0 & R^T \end{bmatrix} \quad (13)$$

where the distributed wrenches are defined in the fixed frame and  $Ad_g^*$  orients the wrenches in the fixed frame to the body frame. For example, the gravity wrench would be  $\bar{\mathbf{W}}_e = \rho A [\hat{\boldsymbol{p}} \boldsymbol{g}, \boldsymbol{g}]^T$ , where  $\boldsymbol{g}$  is the gravitational acceleration vector.

By rearranging Eq. (4) to solve for the force in an individual TCA,  $F_i$ , we can derive the distributed wrench for the TCAs in the fixed frame:

$$\bar{\mathbf{W}}_{act} = \sum_{i=1}^N \begin{bmatrix} \hat{\boldsymbol{p}}_{a,i} F_i(\delta_i, T_i) \boldsymbol{t}'_{a,i} \\ F_i(\delta_i, T_i) \boldsymbol{t}'_{a,i} \end{bmatrix} \quad (14)$$

where  $N$  is the number of TCAs present (in our case  $N = 3$ ),  $\delta_i$  is the  $i$ th TCA's displacement,  $\boldsymbol{t}_{a,i}$  is the unit tangent vector to the  $i$ th TCA and  $\boldsymbol{p}_{a,i}$  is the position of the  $i$ th TCA. The unit tangent vector is defined as  $\boldsymbol{t}_{a,i} = \boldsymbol{p}'_{a,i} / \|\boldsymbol{p}'_{a,i}\|$ . The

derivative of the tangent vector and the value of the actuator position can be obtained as:

$$\boldsymbol{t}'_{a,i} = -\frac{\widehat{\boldsymbol{p}}'_{a,i}{}^2}{\|\boldsymbol{p}'_{a,i}\|^3} \boldsymbol{p}_{a,i} \quad (15)$$

$$\boldsymbol{p}_{a,i} = \boldsymbol{p} + R \boldsymbol{r}_i \quad (16)$$

where  $\boldsymbol{r}_i$  is the displacement of the  $i$ th TCA from the centerline.

The displacement  $\delta_i$  is defined as the arclength of the TCA minus the original arclength of the TCA:

$$\delta_i = \int_0^L \|\boldsymbol{p}'_{a,i}\| ds - L_i \quad (17)$$

where  $L_i$  is the original length of the actuator in the reference configuration, typically  $L_i = L$ . This  $\delta_i$  term is the source of the coupling between the body and the TCAs as  $\delta_i$  depends on the body deformations and the body deformations depend on  $\delta_i$  because the forces exerted by the TCAs are dependent on the displacements. Note that  $\delta_i$  is only defined over the entire body and that is the only value that is appropriate to use in the determination of the force. In order to solve the dynamics, it is inconvenient to have  $\delta_i$  as an integral as we will want everything in the form of either an ODE in time or a PDE. To resolve this, we introduce a new variable  $\epsilon_i$  that will be of the same form as  $\delta_i$  except it is defined for all  $s$ :

$$\epsilon_i(s) = \int_0^s \|\boldsymbol{p}'_{a,i}\| ds - \frac{L_i}{L} s \quad (18)$$

Now it is possible to take a derivative with respect to both  $s$  and  $t$  to obtain the dynamics equations.

$$\epsilon'_i = \|\boldsymbol{p}'_{a,i}\| - \frac{L_i}{L} \quad (19)$$

$$\dot{\epsilon}'_i = \frac{\boldsymbol{p}'_{a,i} \cdot \dot{\boldsymbol{p}}'_{a,i}}{\|\boldsymbol{p}'_{a,i}\|} \quad (20)$$

where  $\cdot$  is the dot product.

The variable  $\epsilon'_i$  can then be used to solve for  $\delta_i$  by being integrated over  $t$  and over  $s$ . However, this still doesn't fully resolve the issue of  $\delta_i$ 's integral dependence as the value for  $\delta_i$  still needs to be known for computing the forces generated by the TCAs. To resolve this, the value for  $\delta_i$  must be guessed prior to solving the system and then checked if the guess is correct by computing  $\delta_i$  with  $\epsilon_i$ . This forces the numerical solution to use an iterative solver for the system (this will lead to an implicit numerical scheme), but this does not interfere with actually obtaining a solution.

Note that the  $\delta_i$  issue just discussed is an artifact of embedding an actuator in a soft body, causing the deformation of the body and actuator to be coupled. For simpler actuators this phenomena is not necessary to consider, but this approach can be generalized for other cases where the actuation couples with the body deformations.

Now, the system can be fully expressed of a state vector,  $\mathbf{y}$ , defined as

$$\mathbf{y} = \begin{bmatrix} g^\dagger \\ \epsilon' \\ \xi \\ \eta \end{bmatrix} \quad (21)$$

where the  $\dagger$  operator represents the extraction of the angle and position values from the  $g$  matrix ( $g^\dagger = [\theta, \mathbf{p}]^T$ ). The angles,  $\theta$ , extracted from  $g$  are the X-Y-Z Euler angles.

With the state vector  $\mathbf{y}$ , the system can be written in terms of the time derivative for  $\mathbf{y}$

$$\dot{\mathbf{y}} = \begin{bmatrix} (g\hat{\eta})^\dagger \\ \frac{(g\hat{\xi}r_i) \cdot (g(\hat{\eta}\hat{\xi} + \hat{\xi})r_i)}{\|\hat{\xi}r_i\|} \\ \eta' + ad\xi\eta \\ \Gamma^{-1}(\mathbf{W}'_{int} - ad^*_\xi \mathbf{W}_{int} + \bar{\mathbf{W}}_{ext} + ad^*_\eta \Gamma\eta) \end{bmatrix} \quad (22)$$

The system can then be written in function form as  $\dot{\mathbf{y}} = f(\mathbf{y}, \mathbf{y}', t, \mathbf{T})$ . In order to solve this system, the boundary conditions are needed. At the base  $s = 0$  we consider the fixed frame is attached at the bottom of the centerline and the manipulator is fixed at the base, thus  $g(s = 0) = I_4$ ,  $\epsilon_i = 0$ , and  $\eta = \mathbf{0}$ . However, we do not know the value of the strain at the base. We can establish the strain at the tip via a balance between the internal stiffness and the TCAs at the tip cross section. This can be formulated as:

$$\mathbf{W}_{int} = Ad^*_g \sum_{i=1}^N \begin{bmatrix} \hat{\mathbf{p}}_{a,i} F_i(\delta_i, T_i) \mathbf{t}_{a,i} \\ F_i(\delta_i, T_i) \mathbf{t}_{a,i} \end{bmatrix} \quad (23)$$

This equation does not have an analytic solution, and due to the  $\delta_i$  dependence of the system, the value for  $\xi(s = L)$  must be recomputed at every iteration. This makes the system more complex, but it is still fully constrained. Finally, we can always know the condition of the system at  $t = 0$ , and it will typically be in the reference configuration.

### C. Dynamics Numerical Solution

To solve the dynamics,  $\dot{\mathbf{y}} = f(\mathbf{y}, \mathbf{y}', t, \mathbf{T})$  we know that it is necessary to solve the balance of the tip at every iteration as well as check that  $\epsilon_i(L) = \delta_i$  and thus need an implicit integration scheme in time. For this, we use the simplest scheme, the backward Euler method [25]:

$$\mathbf{y}^{(i+1)} = \mathbf{y}^{(i)} + \Delta t f(\mathbf{y}^{(i+1)}) \quad (24)$$

where the superscripts on  $\mathbf{y}$  indicate the sequence in time and  $\Delta t$  is the time step. This method is implicit because both sides of the equation depend on the solution of the next time step's value of  $\mathbf{y}$  and must be solved with an iterative equation solver, which is where the boundary conditions can be incorporated.

Then we need the values for  $\mathbf{y}'$  to be able to substitute them into the system equation, for this we use a Padé approximant as its high accuracy reduces the number of spatial discretization points necessary. The form for this approximation is [25]:

$$\frac{1}{6}(\mathbf{y}'_{i+1} + 4\mathbf{y}'_i + \mathbf{y}'_{i-1}) = \frac{1}{2\Delta s}(\mathbf{y}_{i+1} - \mathbf{y}_{i-1}) \quad (25)$$

where the subscripts represent the  $i$ th point in the discretization and  $\Delta s$  is the spatial discretization step. This approximation is 4th-order or has an error proportional to  $\Delta s^4$ . Since we also have to solve for  $\delta_i$ , we use the trapezoidal rule integration scheme to numerically integrate  $\epsilon'_i$  at each time step.

Each step in the solution of the dynamics can be summarized as follows. Guess the values for  $\delta_i$  and  $\xi$ , then use the current values of  $\mathbf{y}$  to approximate the spatial derivatives with the Padé approximant and compute the time derivatives for each state variable, integrate  $\epsilon'_i$  with the trapezoidal rule, check that the implicit Euler equation is satisfied, that the wrenches at the tip balance, and that the guessed  $\delta_i$  matches the computed value of  $\epsilon_i(L)$ . If these conditions are met, then a solution is found. If not, update the guesses with a root finding method and repeat.

## III. SIMULATIONS

In this section we simulate the dynamic response of the soft manipulator with varied voltage inputs. We will demonstrate the response with constant step inputs, step inputs that switch half way through the simulation, and sinusoidal inputs. With the numerical implementation of the developed models, we can simulate the dynamic responses as shown in Fig. 3. The parameters for the body are:  $L = 4\text{cm}$ ,  $D = 1\text{cm}$ ,  $E = 37.8\text{kPa}$ ,  $\nu = 0.5$ ,  $k = 0.19\text{W}/(\text{m} \cdot \text{K})$ ,  $h = 20\text{W}/(\text{m}^2 \cdot \text{K})$ . For TCAs the coiled length is the same as the body (4 cm), the twisted length is 13 cm, the number of coils is 100, the outer diameter is 1.7 mm, the thermal expansion coefficient is  $5\text{e-}5 \text{m}^2/\text{K}$ , and the elastic modulus is 560 MPa.

Looking at the responses we see fairly intuitive behaviors, indicating the correctness of the proposed dynamic models. The thermal profiles (middle row) show a decaying response to the input voltage. Also, due to the TCAs being embedded in the same body, each TCA is influenced by the other being powered. The influence of the input voltage on each TCA through diffusion of heat will be an important consideration for control in future developments. The angle profiles (bottom row) show that the manipulator does its quickest motion at changes in the voltage inputs, which also correspond to the fastest change in temperature, and has a fairly damped response to the input afterwards. The angles presented are the X-Y-Z Euler angles using the fixed frame shown in Fig. 1a. The right portion of Fig. 3 shows a top view of the tip position through time for the given dynamic responses. In this figure, we can see the drift caused by switching the actuated TCAs and the damped response in the sinusoidal generated path.

## IV. CONCLUSIONS AND FUTURE WORK

In this paper, we demonstrate the modeling of the thermodynamics and mechanics of a soft manipulator using embedded TCAs. To do this, we use standard approaches

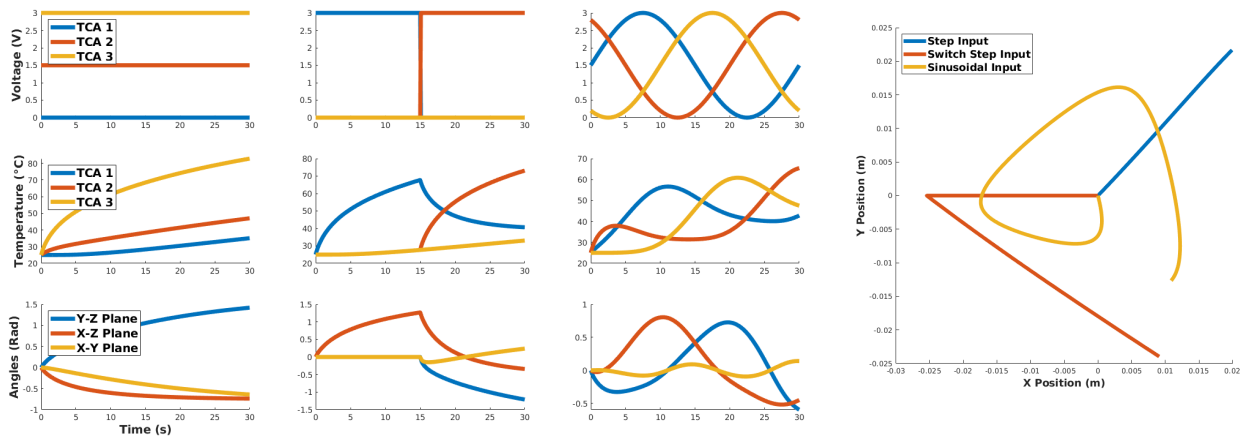


Fig. 3. Left) The simulation results with the voltage input (top row), the thermal response (middle row), and the dynamic response (bottom row) over 30s. Each column shows the result for a specific case: 1) step voltages applied to two TCAs, 2) one TCA being actuated and then switching to another after 15s, 3) a sinusoidal input to two TCAs. The voltage profiles are step inputs of 3V. The thermal responses show the temperature profiles of the individual TCAs over time. The plots of the angles show the angle of the manipulator's tip over time. The angles are rotations in the fixed Y-Z, X-Z, and X-Y plane, which are also the X-Y-Z Euler angles relative to the fixed frame shown in Fig. 1a. Right) the top view of the tip position of the simulations.

to modeling the thermodynamics of a conductive body and a dynamic Cosserat rod model with coupling between the TCAs and the body deformation. The resulting numerical implementations are then tested, and the results of which give reasonable and intuitive results for the forward dynamics. In the future we aim to utilize the developed model for determining control inputs for manipulators like the one analyzed and simulated. We will also leverage machine learning techniques to approximate the dynamics to enable faster computation speed that is necessary for real-time control.

## REFERENCES

- [1] D. Rus and M. T. Tolley, "Design, fabrication and control of soft robots," *Nature*, vol. 521, no. 7553, pp. 467–475, May 2015, insight.
- [2] Y. Elsayed, A. Vincensi, C. Lekakou, T. Geng, C. Saaj, T. Ranzani, M. Cianchetti, and A. Menciassi, "Finite element analysis and design optimization of a pneumatically actuating silicone module for robotic surgery applications," *Soft Robotics*, vol. 1, no. 4, pp. 255–262, 2014.
- [3] P. Polygerinos, Z. Wang, K. C. Galloway, R. J. Wood, and C. J. Walsh, "Soft robotic glove for combined assistance and at-home rehabilitation," *Robotics and Autonomous Systems*, vol. 73, pp. 135–143, 2015.
- [4] M. T. Tolley, R. F. Shepherd, B. Mosadegh, K. C. Galloway, M. Wehner, M. Karpelson, R. J. Wood, and G. M. Whitesides, "A resilient, untethered soft robot," *Soft robotics*, vol. 1, no. 3, pp. 213–223, 2014.
- [5] S. Neppalli, M. A. Csencsits, B. A. Jones, and I. D. Walker, "Closed-form inverse kinematics for continuum manipulators," *Advanced Robotics*, vol. 23, no. 15, pp. 2077–2091, 2009.
- [6] D. Trivedi, A. Lotfi, and C. D. Rahn, "Geometrically exact models for soft robotic manipulators," *IEEE Transactions on Robotics*, vol. 24, no. 4, pp. 773–780, Aug 2008.
- [7] M. Giorelli, F. Renda, M. Calisti, A. Arienti, G. Ferri, and C. Laschi, "A two dimensional inverse kinematics model of a cable driven manipulator inspired by the octopus arm," in *2012 IEEE International Conference on Robotics and Automation*, May 2012, pp. 3819–3824.
- [8] W. McMahan, B. Jones, I. Walker, V. Chitrakaran, A. Seshadri, and D. Dawson, "Robotic manipulators inspired by cephalopod limbs," *Proceedings of the Canadian Engineering Education Association*, 2011.
- [9] D. C. Rucker and R. J. W. III, "Statics and dynamics of continuum robots with general tendon routing and external loading," *IEEE Transactions on Robotics*, vol. 27, no. 6, pp. 1033–1044, Dec 2011.
- [10] C. A. Daily-Diamond, A. Novelia, and O. M. O'Reilly, "Dynamical analysis and development of a biologically inspired sma caterpillar robot," *Bioinspiration & biomimetics*, vol. 12, no. 5, p. 056005, 2017.
- [11] S.-W. Yeom and I.-K. Oh, "A biomimetic jellyfish robot based on ionic polymer metal composite actuators," *Smart materials and structures*, vol. 18, no. 8, p. 085002, 2009.
- [12] K. Jung, J. C. Koo, Y. K. Lee, H. R. Choi *et al.*, "Artificial annelid robot driven by soft actuators," *Bioinspiration & biomimetics*, vol. 2, no. 2, p. S42, 2007.
- [13] S. M. Mirvakili and I. W. Hunter, "Artificial muscles: Mechanisms, applications, and challenges," *Advanced Materials*, 2017.
- [14] C. S. Haines, M. D. Lima, N. Li, G. M. Spinks, J. Foroughi, J. D. Madden, S. H. Kim, S. Fang, M. J. de Andrade, F. Göktepe *et al.*, "Artificial muscles from fishing line and sewing thread," *science*, vol. 343, no. 6173, pp. 868–872, 2014.
- [15] A. Abbas and J. Zhao, "A physics based model for twisted and coiled actuator," in *Robotics and Automation (ICRA), 2017 IEEE International Conference on*. IEEE, 2017, pp. 6121–6126.
- [16] B. A. Jones and I. D. Walker, "Kinematics for multisection continuum robots," *IEEE Transactions on Robotics*, vol. 22, no. 1, pp. 43–55, Feb 2006.
- [17] I. Robert J. Webster and B. A. Jones, "Design and kinematic modeling of constant curvature continuum robots: A review," *The International Journal of Robotics Research*, vol. 29, no. 13, pp. 1661–1683, 2010.
- [18] F. Renda, V. Cacucciolo, J. Dias, and L. Seneviratne, "Discrete cosserat approach for soft robot dynamics: A new piece-wise constant strain model with torsion and shears," in *Intelligent Robots and Systems (IROS), 2016 IEEE/RSJ International Conference on*. IEEE, 2016, pp. 5495–5502.
- [19] D. C. Rucker, B. A. Jones, and R. J. Webster, "A model for concentric tube continuum robots under applied wrenches," in *Robotics and Automation (ICRA), 2010 IEEE International Conference on*. IEEE, 2010, pp. 1047–1052.
- [20] F. Boyer, M. Porez, and W. Khalil, "Macro-continuous computed torque algorithm for a three-dimensional eel-like robot," *IEEE Transactions on Robotics*, vol. 22, no. 4, pp. 763–775, 2006.
- [21] F. Renda, M. Giorelli, M. Calisti, M. Cianchetti, and C. Laschi, "Dynamic model of a multibending soft robot arm driven by cables," *IEEE Transactions on Robotics*, vol. 30, no. 5, pp. 1109–1122, 2014.
- [22] T. L. Bergman and F. P. Incropera, *Fundamentals of heat and mass transfer*. John Wiley & Sons, 2011.
- [23] A. Abbas and J. Zhao, "Twisted and coiled sensor for shape estimation of soft robots," in *2017 IEEE/RSJ International Conference on Intelligent Robots and Systems (IROS)*, Sept 2017, pp. 482–487.
- [24] J. Linn, H. Lang, and A. Tuganov, "Geometrically exact cosserat rods with kelvin-voigt type viscous damping," *Mechanical Sciences*, vol. 4, no. 1, pp. 79–96, 2013.
- [25] H. Lomax, T. H. Pulliam, and D. W. Zingg, *Fundamentals of computational fluid dynamics*. Springer Science & Business Media, 2013.